Methodology to design mobile-based camera lenses using freeform surfaces

Zhuang, Zhenfeng, Dallaire, Xavier, Parent, Jocelyn, Roulet, Patrice, Thibault, Simon

Zhenfeng Zhuang, Xavier Dallaire, Jocelyn Parent, Patrice Roulet, Simon Thibault, "Methodology to design mobile-based camera lenses using freeform surfaces," Proc. SPIE 11814, Current Developments in Lens Design and Optical Engineering XXII, 1181403 (1 August 2021); doi: 10.1117/12.2594001

SPIE.

Event: SPIE Optical Engineering + Applications, 2021, San Diego, California, United States

Methodology to design mobile-based camera lenses using freeform surfaces

Zhenfeng Zhuang[1], Xavier Dallaire[1], Jocelyn Parent[1], Patrice Roulet[1], Simon Thibault[1,2]
[1]Immervision Inc, 2020 Robert-Bourassa Blvd., Suite 2320, Montreal, Quebec, H2A 2A5 Canada
[2]Centre d'optique, photonique et laser, Département de physique, de génie physique et d'optique, Université Laval, 2375, rue de la Terrasse, Québec G1V 0A6, Canada

ABSTRACT

Freeform technology is one of the most promising solutions for enhancing the capability of aberration correction and improving performance of optical systems. Aiming to demonstrate the freedom and flexibility of optical system design, several challenging design examples using freeform surface are presented, including two wide-angle camera lenses adopting even and odd pedal polynomial formulations for symmetric optical surface description, and an anamorphic cinema lens employing non-rotationally symmetric surfaces for capturing a wider aspect ratio and offering a 1.33× squeeze factor on a 4:3 sensor size. Methods and constraints for designing and optimizing the optical systems are discussed. The optical performances of these design examples are analyzed and the results verify the practicability and effectiveness of the proposed formulations and design strategies in the field of freeform imaging optical design.

Keywords: Lens system design, optical systems, geometric optical design, aspherics

1. INTRODUCTION

Freeform optics has attracted much attention from optical engineers owning to its unique features in manipulating rays by carefully using designed the surface shapes, which are defined as variables, such as control points, coefficients, vectors and so on. Compared to conventional spherical or aspherical surfaces, freeform surfaces afford higher degrees of freedom in optical design and contribute to superior performance on account of the flexibility of arbitrary surface shapes. Therefore, freeform surfaces have been widely implemented to realize complex irradiance distributions [1-3] as well as to enhance image quality in imaging optical systems [4-6].

In the most general meaning, the term "optical freeform" is used to refer to surface non-linear surfaces or those without rotational symmetry. To provide specific clarification, the complex rotationally symmetric surface description can be classified as a freeform surface, in comparison with conventional aspheric surface. There are three main methods to realize the freeform optical design. The first one is to take a direct method by calculating the surface normals with the incident ray as well as the emergent ray [7,8]. The discrete points are fitted as a starting point, and then further optimized in combination with classical optimization methods. However, this method is often unpractical in finding the optimum solution and leads to inconsistent results. The second solution is to combine pre-defined surface descriptions with classic optical systems [6,9,10], for example: Qbfs asphere, Zernike polynomial, xy polynomial, or non-uniform rational B-splines (NURBS). Numerous analyses and applications were conducted with these freeform surfaces. However, the studies revealed the appalling level of dependence on the starting points about state-of-the-art freeform optical design methods. Another means of is to consider alternative freeform surface representations. Cakmakci presented an optical surface representation considering local basis functions [11]. A modified Zernike polynomial was introduced to represent tilt surfaces [12]. A Nagata patch, including form errors of fabrication processes, was adopted to stand for the description of optical surfaces [13].

In this work, we present a pedal-based freeform surface representation specially developed for replacing the S-shaped optical element that is the most frequently utilized in the mobile-based camera lens. Our representation combines a base surface and a pedal-based polynomial function. The schemes are implemented in the mobile-based camera lens design. Two design examples that integrate an extended odd pedal-based freeform surface and even pedal-based freeform surface are offered. Also, an anamorphic cinema lens using xy polynomial surfaces is introduced. Design strategies, including discussion of constraints and downsides of conventional rotationally symmetric optical system are proposed. The application of this method for designing a miniature cinematic lens is illustrated, and the image quality is evaluated and analyzed.

Current Developments in Lens Design and Optical Engineering XXII, edited by R. Barry Johnson, Virendra N. Mahajan, Simon Thibault, Proc. of SPIE Vol. 11814, 1181403 · © 2021 SPIE
CCC code: 0277-786X/21/$21 · doi: 10.1117/12.2594001

2. CAMERA LENS USING SYMMETRICAL PEDAL-BASED FREEFORM SURFACE

2.1 Representation methods for freeform surfaces with form resembling

A pedal-curve is identical to the S-shaped aspheric surfaces that are regularly adopted in mobile-based optical system. The surface sag of the pedal-curve can be determined as [14]:

$$S = b - \sqrt{\frac{b^2 - 2r^2 + \sqrt{b^4 + 4(a^2 - b^2)r^2}}{2}} \tag{1}$$

where a and b are the semi-major and semi-minor axis of the pedal curve, respectively. $r = \sqrt{x^2 + y^2}$ is the radial coordinate of the surface. Similar to the construction of the extended odd aspheric surface, the sag of the freeform surface can be represented as a base surface with a linear combination of pedal function. The base surface is commonly a conic surface, thus, Eq. (1) can be expressed as [15]:

$$Z_{(r)} = \frac{cr^2}{1 + \sqrt{1 - (1 + k)c^2 r^2}} + \sum_{i=1}^{n} A_i S^i \tag{2}$$

where R=1/c is the radius of curvature of the surface, k is the conic constant, and S^i is the i'th order pedal function and A_i is the corresponding coefficient. User defined surface (UDS) offers an approach to define any surface that can be described as an explicit mathematical function form Z=F(x,y). An odd pedal-based freeform surface is programmed using C language and then compiled to a custom dynamic link library (DLL) file to be used in commercial optical design software. Figure 1 provides the lens data editor (LDE), using an odd pedal-based freeform surface in commercial optical design software. The "#Terms" is used to specify the maximum term to be used in calculating the surface sag. The maximum term of pedal function is 30 in our design study.

a	b	# Terms	1st Order Term	2nd Order Term	3rd Order Term	4th Order Term	5th Order Term	6th Order Term	7th Order Term	8th Order Term
17.5159	6.2133	8.0000	-0.0369	-0.9614	-1.3076	-7.0665	-14.3799	-11.4264	6.1516	8.8285

Figure 1. Illustration of LDE of ZEMAX with extended odd pedal-based freeform surface.

Furthermore, an even polynomial can be constructed for characterizing the pedal-based freeform surface. The even polynomial has a similar construction to the even aspheric surface, as expressed in:

$$Z_{(r)} = \frac{cr^2}{1 + \sqrt{1 - (1 + k)c^2 r^2}} + A_1 S^2 + A_2 S^4 + A_3 S^6 + \cdots + A_{10} S^{20} \tag{3}$$

The same scheme is also implemented to characterize the proposed even pedal-based freeform surface. The LDE of using an even pedal-based freeform surface in commercial optical design software is demonstrated in Fig. 2.

a	b	2nd Order Term	4th Order Term	6th Order Term	8th Order Term	10th Order Term	12th Order Term	14th Order Term	16th Order Term	18th Order Term	20th Order Term
24.8594	9.7268	-2.2692	0.3772	-14.4188	39.3707	0.0000	0.0000	0.0000	0.0000	0.0000	0.0000

Figure 2. Illustration of LDE of ZEMAX with an even pedal-based freeform surface.

2.2 Design examples

We will demonstrate the design procedures of a mobile-based camera lens with the proposed extended odd and even pedal-based freeform surfaces in detail to show the effectiveness of our scheme. The design starting point and target specifications are presented in Fig. 3 and Table 1, respectively. As shown in Fig. 3, the camera lens consists of 6 pieces of plastic aspherical element, including one S-shaped optical element. Also, the aperture stop is placed between the first and the second optical elements. The 1/3.09-inch CMOS sensor with an active area 4.656 mm × 3.496 mm and a resolution of 16.28 Mega pixels is chosen to ensure a compact package size as well as sufficient resolution. The mobile-based camera

lens is aiming to provide wide angle field of view (FoV) around 120°~125°, and the f-number is around 2.0 to the performance of enhancing low-light images.

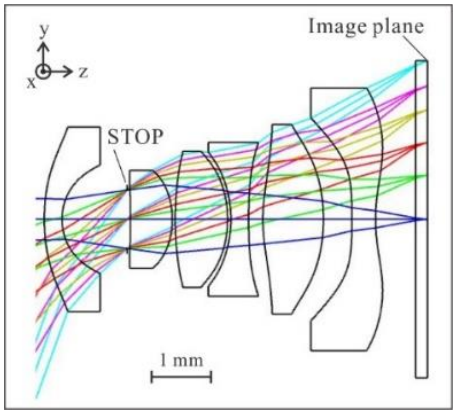

Figure 3. Starting point of the optical system.

Table 1. The target specifications of the mobile-based camera lens.

Parameters	Values
f-number	2.0
Diagonal FoV	120° ~ 125°
Total length	≤5.5 mm
Working spectrum	486nm ~ 656 nm
Sensor size	1/3.09”
Active area of sensor	4.656 mm × 3.496 mm

The optimization process can be mainly divided into two steps. The first step of using the starting point of the camera lens is to correct primary aberrations and meet the target specifications by adopting aspheric surfaces. The second step is further optimizing the system to enhance the imaging quality by employing the proposed pedal-based freeform surfaces. During the optimization process, the S-shaped aspheric surface is converted to pedal-based freeform surface one by one aiming to afford reliable convergence during the optimization process. Meanwhile, we utilize the least squares fitting algorithm to obtain a close-fitting pedal-based freeform surface.

In the first example, a highly compact camera lens with well-performing imaging quality is designed by extended odd pedal-based freeform surfaces to meet stringent design requirements. Figure 4(a) depicts the layout of the optimized extended odd pedal-based freeform camera lens. The designed camera lens utilizes eight even aspheric surfaces and four extended odd pedal-based freeform surfaces. The FoV of the optical system is 121°, the f-number is 2.06, and the total track of the length is about 5.4mm, which demonstrates a compact package size. The modulation transfer function (MTF) values of all the fields shown in Fig. 4(b) are greater than 0.19 at 220 lp/mm. The distortion grid of the optical system is illustrated in Fig. 4(c). The maximum distortion is about 24.7%. It should be emphasized that the image distortion is challenging to correct due to the large FoV. Nevertheless, it can be further corrected by employing an image-processing algorithm.

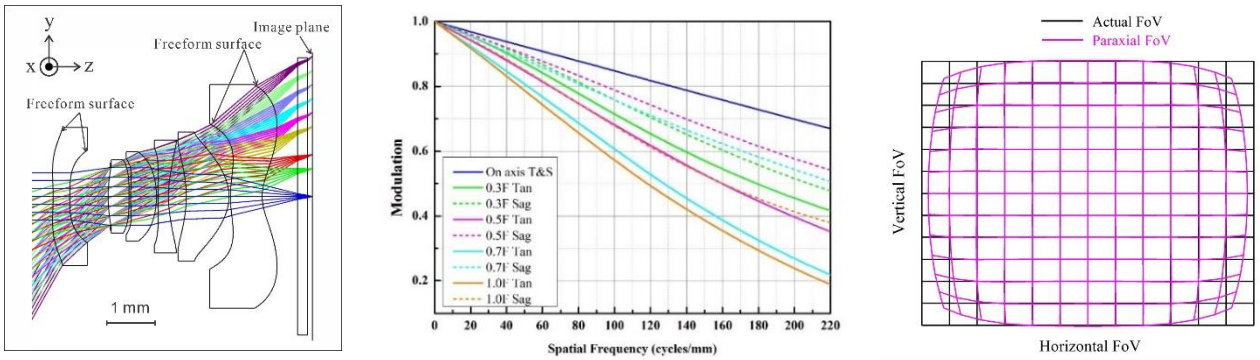

(a) (b) (c)

Figure 4. (a) Optical layout; (b) polychromatic MTF plots and (c) distortion grid for the extended odd pedal-based freeform camera lens.

To verify the roughness of the proposed freeform surface description, in the second example, we further design a mobile-based camera lens using an even pedal-based freeform surface. The final even pedal-based freeform camera lens is obtained after optimization, as shown in Fig. 5(a). The freeform surfaces are placed at the first surface of the first element as well as the first and second surfaces of the last element. The FoV of the optical system is 121°, the f-number is 2.06, and the total track of the length is about 5.3mm. Figure 5(b) illustrates the MTF of the freeform camera lens after utilizing freeform surfaces. The distortion grid of the freeform camera lens is shown in Fig. 5(c), and its maximum distortion is about 24.4%.

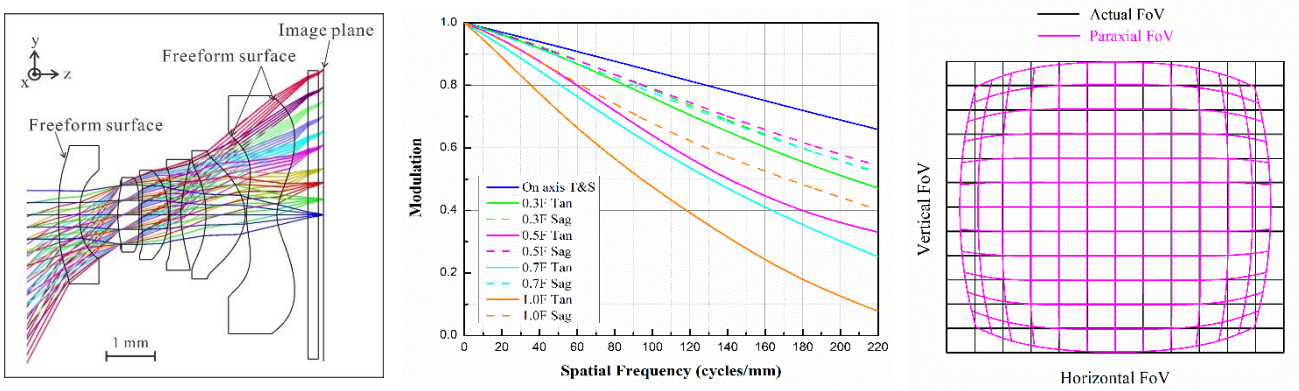

(a) (b) (c)

Figure 5. (a) Optical layout; (b) polychromatic MTF plots and (c) distortion grid for the even pedal-based freeform camera lens.

3. ANAMORPHIC CINEMA LENS USING ASYMMETRICAL FREEFROM SURFACE

3.1 Statement of the problem

A rotationally symmetric optical system produces an image with 1.33 aspect ratio when capturing with a 4:3 aspect ratio sensor. 16:9 is the standard for most digital cameras in video mode and it is the most popular format of the video. It is critical to display clear and undistorted video images for the 16:9 aspect ratio. There are two ways to display 16:9 video on a 4:3 video source, and some certain compromises are required. As shown in Fig. 6(a), black bars are added on the left and right sides of the displayed image. Alternatively, the displayed image should be cropped from the picture or video to meet the 16:9 wide screen movie format requirement because the camera aspect ratio 4:3 does not match the wide screen aspect ratio, as demonstrated in Fig. 6(b). It means masking the top and bottom of each frame, thus sacrificing vertical resolution and vertical FoV are inevitable.

Nevertheless, because of the unique characteristics, anamorphic lens should be a good means to provide a 1.77:1 ratio in a 4:3 aspect format without sacrificing resolution. To produce a 16:9 wide screen image or movie, a 1.33× anamorphic

lens is required. To achieve this, compared with the traditional rotationally symmetric optical system, the anamorphic lens squeezes the horizontal information from the user's scene to fit the constraint of the sensor's physical size. However, an anamorphic set is usually used in conjunction with the main camera, which enables the capture of a wide screen image format in a 4:3 aspect ratio. It would be extremely desirable to develop a cinematic lens in mobile-based applications.

Figure 6. Widescreen image captured on a 4:3 aspect ratio sensor with a rotationally symmetric lens. (a) the black bars are added on the left and right sides to accommodate 16:9 wide screen video format; (b) the top and bottom of the image go unused to accommodate a super wide-angle image 4:3 to 16:9 wide screen movie format.

3.2 Design strategy

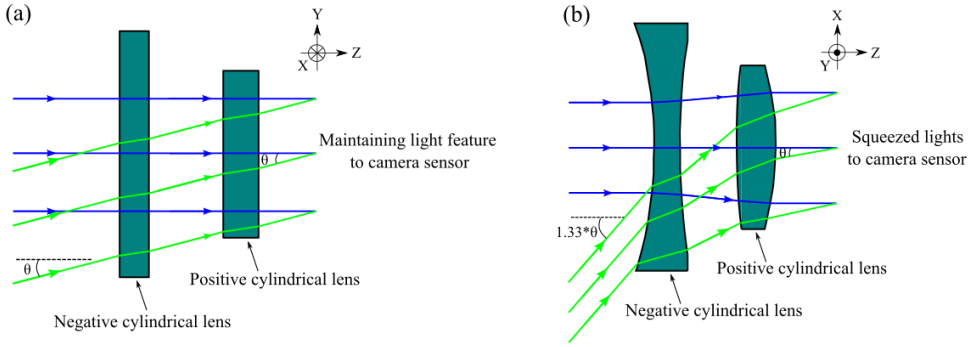

Figure 7. Illustration of the FoV (a) maintaining in the vertical direction and (b) suppression in the horizontal direction.

As mentioned above, the feature of the anamorphic lens is aimed at compressing horizontal information from the user scene, while maintaining the same vertical information. Considering the simplistic anamorphic lens; it comprises of two groups of optical elements with double curvature surfaces, which have different radii of curvature in two perpendicular symmetry planes, such as cylindrical surface, toroidal surface, gradient index optics or different prism pairs. The design methodology of an anamorphic lens is shown in Fig. 7. It demonstrates the operating principle of the strategy for capturing more horizontal information with double curvature surfaces. It is indicated that the lens group possesses no power in y-z plane and optical power in x-z plane. Incorporating the double curvature surfaces group into the camera lens enables it to be capable of meeting the constraint of squeezing a horizontal scene within a certain ratio. For a mobile-based cinematic lens, the anamorphic ratio (AR) is defined as the ratio of the system focal lengths in the orthogonal x-z and y-z planes of symmetry in the paraxial approximation:

$$AR_{paraxial} = \frac{f_{xoz}}{f_{yoz}} \tag{4}$$

Due to the influence of aberrations, there is a variation on AR if the non-paraxial approximation. In the object space, each field can be described by (θ_x, θ_y), which are the angles between the bundle of rays and the system axis. Many bundles of

rays with different directions enter the imaging system and reach the detector. Each position can be described by (h_x, h_y), which is the lateral position of the corresponding ray at the image plane. Thus, any ray entering the imaging system can be solely described by a mapping from (θ_x, θ_y) to (h_x, h_y). For a given field indexed as (i, j), each focal length in x- and y-directions of its corresponding image position can be expressed as:

$$\begin{cases} f_{x(i,j)} = \dfrac{H_{x(i,j)}}{\tan\left(\theta_{x(i,j)}\right)} \\ f_{y(i,j)} = \dfrac{H_{y(i,j)}}{\tan\left(\theta_{y(i,j)}\right)} \end{cases} \tag{5}$$

From Eq. (5), we obtain the AR for a specified filed:

$$AR_{(i,j)} = \frac{f_{x(i,j)}}{f_{y(i,j)}} \tag{6}$$

3.3 Design example and optical performance analysis

In our study, to realize optical powers differently along different axes, an xy polynomial is employed to generate different optical powers in two orthogonal planes of symmetry. The double curvature surface is symmetric about the XOZ and YOZ planes respectively, so the odd power coefficients of x and y in the polynomial are set to zeros, therefore, the expression of the polynomial is:

$$Z = \frac{cr^2}{1 + \sqrt{1 - (1+k)c^2r^2}} + a_{02}x^0y^2 + a_{20}x^2y^0 + a_{04}x^0y^4 + a_{22}x^2y^2 + a_{40}x^4y^0 + \cdots \tag{7}$$

where the a_{02}, a_{20}, a_{04}, a_{22}, and a_{40} are the term coefficients in the xy polynomial expression.

A promising starting point for mobile-based cinematic lens is lacking. Moreover, by taking the speed and convergence aspects into consideration, we adopt the following design strategy. In the first step of optimization, the AR under the paraxial approximation needs to be achieved, avoiding any stagnation. Only the biased fields along the tangential and sagittal directions are sampled. The cylindrical surfaces are adopted to obtain a certain AR. The other surfaces are aspherical surfaces to correct first-order aberrations. Following the intermediate stage of optimization, the cylindrical type surfaces are replaced with anamorphic aspheric surfaces, and the radii in the vertical direction are also set as variables to correct the aberrations in this direction. The sample fields are added across the entire FoV as the optimization process progressed. At the final stage of optimization, the anamorphic aspheric surfaces are converted to xy polynomial surface to further improve the image quality of the system.

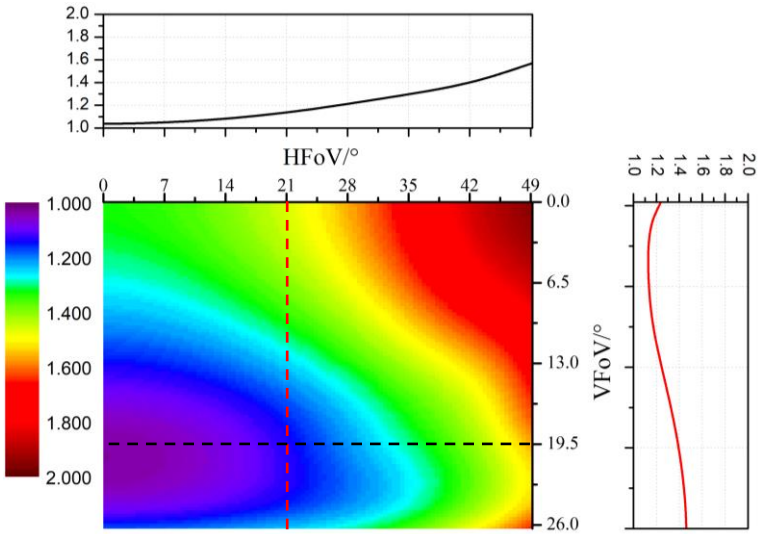

Figure 8. AR at each field position for the cinematic lens design. The top panel is the AR sliced along the x axis with y = 19.5°, and the right panel is the AR sliced along the y axis with x = 21°.

To quantitatively analyze the performance of the cinematic lens, the image quality is assessed. Because of the symmetry of the freeform lens, only one quadrant is plotted. The horizontal field and the vertical field are divided into 21 by 21. Following Eqs. (5)-(6), the AR is calculated. Figure 8 shows the two-dimensional (2D) various AR distribution of the cinematic lens. With the design AR of 1.33 for the anamorphic cinema lens, our results correspond to a range of AR between 1.01 and 1.99 due to the variation of distortion across the entire FoV. The AR is about 1.33 at the center FoV, and the ratio increases as it approaches to the peripheral field along the horizontal FoV. Nevertheless, this ratio reduces as it nears to the edge field along the vertical FoV. The red line represents the AR is computed along the x = 21°, the AR is varied from 1.11 to 1.46; and the black line represents the AR which is computed along y = 19.5°. It rises from 1.02 to 1.58. As shown in Fig. 9, the tangential MTF and sagittal MTF are mapped across the full field at 110 lp/mm spatial frequency. The MTF values are over 0.45 at 0.8 field. It is demonstrated that the MTFs are gradually diminishing across the entire FoV. Thus, the smoothness of the MTF indicates that the xy polynominal surface is smooth over the entire FoV.

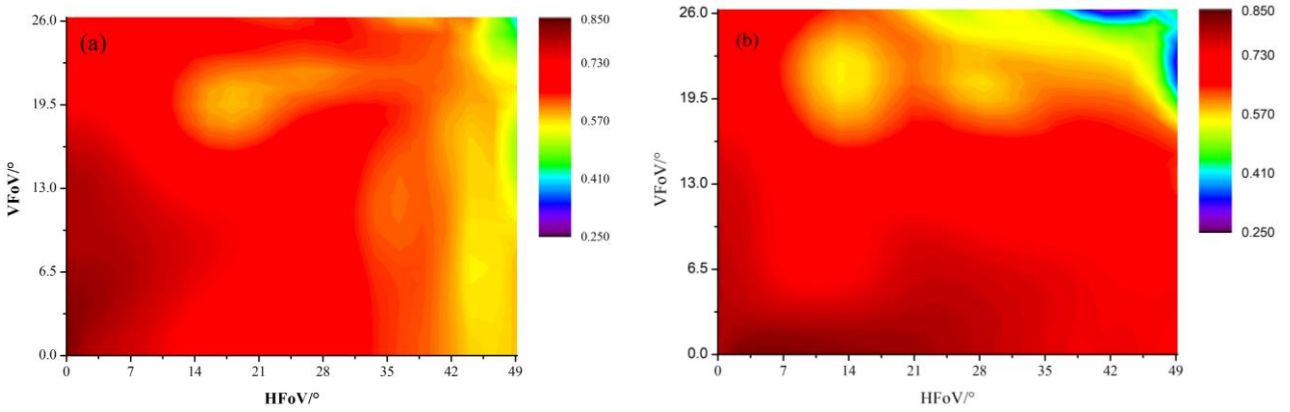

Figure 9. Field map of (a) Tangential MTF and (b) sagittal MTF for mobile-based cinematic lens.

Figure 10 further demonstrates 2D relative illumination (RI), which is calculated as the ratio of the peripheral intensity to the central intensity. It can be observed that due to the wide FoV and large image size, the RI can be significantly decreased. Figure 10(a) gives the RI along the x=0 mm and y = 0 mm. As illustrated in this figure, the RI value, which is denoted by blue line, is over 44.3% along x=0 mm, while the RI value which is represented by red line, is over 27% along y=0 mm. The RI as a function of diagonal FoV is shown in Fig. 10(b). The RI value in the peripheral field is over 15.9%.

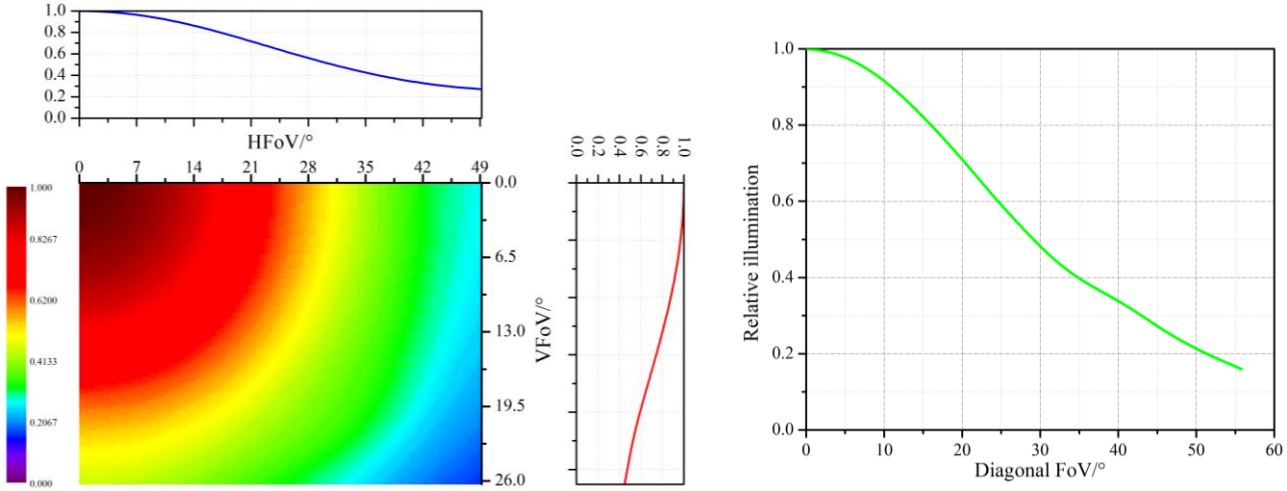

Figure 10. (a) Relative illumination produced by the cinematic lens, and the corresponding relative illumination curves along the lines x = 0 mm and y = 0 mm; (b) the corresponding relative illumination along diagonal FoV.

The root-mean-square (RMS) spot size has been using as one of the main factors in considering the superposition of primary and high order aberrations. The RMS spot size is assessed over the full FoV as shown in Figure 11(a). The RMS spot radii is within the range of 0 μm to 6μm and the maximum spot radius appears at the corner field. Additionally, one of the key parameters of the camera lens for mobile applications is lateral color, which is defined as:

$$\Delta Z_{F-C} = \sqrt{(x_F - x_C)^2 + (y_F - y_C)^2} \tag{8}$$

where $(x_F,\ y_F)$ represents the position of the principal rays for blue light at the image plane, and $(x_C,\ y_C)$ denotes the position of the principal rays for red light at the image plane. According to Eq. (8), we can calculate the lateral color field map, as shown in Fig. 11(b). The lateral color ranges from 0 to 4.4 μm over the full FoV. The result shows that a large lateral color occurs at the marginal region along x = 0 mm. A small lateral color on the marginal region along y = 0mm is offered for this design.

As demonstrated above, the proposed design strategy and optimization approach yield a promising design of a high-performance mobile-based cinematic lens.

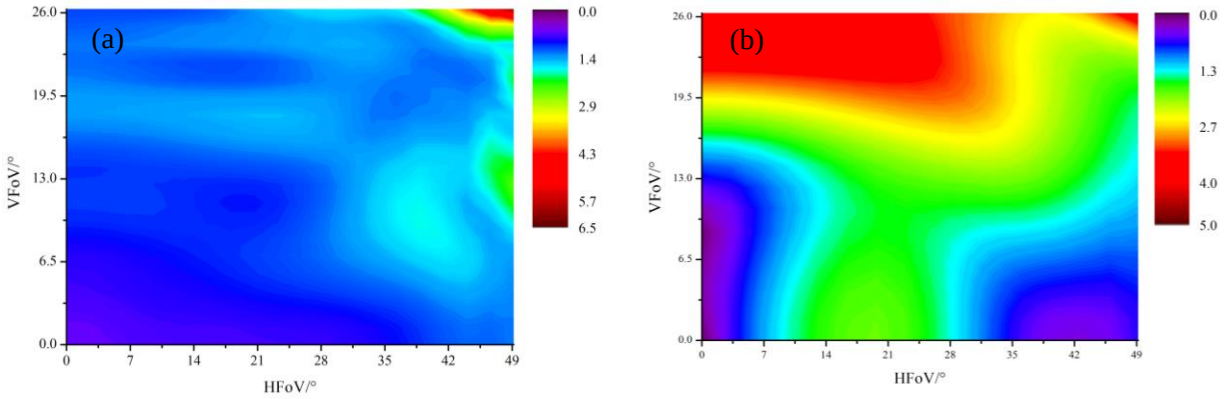

Figure 11. (a) RMS spot size and (b) lateral color field maps for the cinematic lens.

4. CONCLUSIONS

In conclusion, we developed a geometric shape modeling scheme to represent the symmetric freeform optical surface in mobile-based camera lens, which includes at least one S-shaped element. Associated with the S-shaped modeling scheme, the superiority was demonstrated in two challenging design cases utilizing odd and even pedal-based symmetric freeform surfaces. Also, we reported a mobile-based camera lens using anamorphic freeform surfaces with 1.33× AR in the paraxial calculation. The detailed two-dimensional image qualities were illustrated and discussed. We expect that this design is particularly attractive for utilization in the motion picture industry.

REFERENCES

[1] R. Wu. L. Yang, Z. Ding, L. Zhao, D. Wang, K. Li, F. Wu, Y. Li, Z. Zheng, and X. Liu, "Precise light control in highly tilted geometry by freeform illumination optics," Opt. Lett. 44(11), 2887-2890 (2019).

[2] D. A. Bykov, L. L. Doskolovich, A. A. Mingazov, and E. A. Bezus, "Optics mass transportation problem in the design of freeform optical elements generating far-field irradiance distributions for plane incident beam," Appl. Opt. 58(33), 9131-9140 (2019).

[3] X. Mao, S. Xu, X. Hu, and Y. Xie, "Design of a smooth freeform illumination system for a point light source based on polar-type optimal transport mapping," Appl. Opt. 56(22), 6324-6331 (2017).

[4] J. Stock, A. Broemel, J. Hartung, D. Ochse, and H. Gross, "Description and reimplementation of real freeform surfaces," Appl. Opt. 56(3), 391-396 (2017).

[5] Y. Nie, R. Mohedano, P. Benitez, J. Chaves, J. Minano, H. Thienpont, and F. Duerr, "Multifield direct design method for ultrashort throw ratio projection optics with two tailored mirrors," Appl. Opt. 55(14), 3794-3800 (2016).

[6] Z. Zhuang, Y. Chen, F. Yu, and X. Sun, “Field curvature correction method for ultrashort throw ratio projection optics design using an odd polynomial mirror surface,” Appl. Opt. 53(22), E69-E76 (2014).
[7] D. Cheng, Y. Wang, and H. Hua, “Freeform optical system design with differential equations,” Proc. SPIE. 7849, 78490Q (2010).
[8] Y. Nie, H. Thienpont, and F. Duerr, “Multi-fields direct design approach in 3D: calculating a two-surface freeform lens with an entrance pupil for line imaging systems,” Opt. Express 23(26), 34042-34054 (2015).
[9] G. W. Forbes, “Characterizing the shape of freeform optics,” Opt. Express. 20(3), 2483-2499 (2012).
[10] P. Jester, C. Menke, and K. Urban, “B-spline representation of optical surfaces and its accuracy in a ray trace algorithm,” Appl. Opt. 50(6), 822-828 (2011).
[11] O. Cakmakci, B. Moore, H. Foroosh, and J. P. Rolland, “Optimal local shape description for rotationally non-symmetric optical surface design and analysis,” Opt. Express 16(3), 1583-1589 (2008).
[12] A. Yabe, “Representation of freeform surfaces suitable for optimization,” Appl. Opt. 51(15), 3054-3058 (2012).
[13] S. Morita, Y. Nishidate, T. Nagata, Y. Yamagata, and C. Teodosiu, “Ray-tracing simulation method using piecewise quadratic interpolant for aspheric optical systems,” Appl. Opt. 49(18), 3442-3451 (2010).
[14] Y. F. Yan, and J. Sasian, “Miniature camera lens design with a freeform surface,” Proc. SPIE 10590, 1059012 (2017).
[15] Z. Zhuang, X. Dallaire, J. Parent, P. Roulet, and S. Thibault, “Geometrical-based quasi-aspheric surface description and design method for miniature, low-distortion, wide-angle camera lens,” Appl. Opt. 59(27), 8408-8417 (2020).